Letter

Superconducting instabilities in a spinful Sachdev-Ye-Kitaev model

Étienne Lantagne-Hurtubise, Vedangi Pathak, Sharmistha Sahoo, and Marcel Franz

Department of Physics and Astronomy, Stewart Blusson Quantum Matter Institute, University of British Columbia, Vancouver, British Columbia, Canada V6T 1Z4

(Received 7 January 2021; revised 9 June 2021; accepted 22 June 2021; published 23 July 2021)

We introduce a spinful variant of the Sachdev-Ye-Kitaev model with an effective time-reversal symmetry, which can be solved exactly in the limit of a large number N of degrees of freedom. At low temperature, its phase diagram includes a compressible non-Fermi liquid and a strongly correlated spin singlet superconductor that shows a tunable enhancement of the gap ratio predicted by BCS theory. These two phases are separated by a first-order transition, in the vicinity of which a gapless superconducting phase, characterized by a nonzero magnetization, is stabilized upon applying a Zeeman field. We study equilibrium transport properties of such superconductors using a lattice construction and propose a physical platform based on topological insulator flakes where they may arise from repulsive electronic interactions.

DOI: 10.1103/PhysRevB.104.L020509

Understanding strongly correlated forms of superconductivity (SC), going beyond the celebrated Bardeen-Cooper-Schrieffer (BCS) [1–3] and Migdal-Eliashberg [4–7] theories, remains an ongoing avenue of research. One of the main difficulties lies in the rarity of tractable models [8–10] providing analytical insight into this phenomenon. Recently, the advent of exactly solvable models of non-Fermi liquids, the family of so-called Sachdev-Ye-Kitaev (SYK) models [11–14], has sparked remarkable progress in exploring correlated phases with intriguing properties such as strange metallic transport and maximal chaos [15–24]. Solvable models of correlated superconductors have been similarly constructed—two popular approaches consisting of explicitly adding pairing terms to an SYK construction [25–27] or considering random Yukawa electron-phonon interactions [28–32].

Building on these ideas, in this Letter we introduce a simple model for correlated superconductivity with rich phenomenology where the superconducting correlations are instead generated directly by disordered SYK-type fermionic interactions [33,34]. It consists of a pair of coupled complex SYK (cSYK) models [11,12,35] with random two-body interactions that are constrained by an antiunitary time-reversal symmetry, and can thus be regarded as a *spinful* generalization of the SYK model. This is inspired by recent work on a related but subtly different symmetry setting where two SYK models are instead related by a unitary symmetry [36–40], and which hosts both (gapped) symmetry-broken and (gapless) non-Fermi liquid phases with a holographic interpretation.

In analogy with the results of these works, at low temperature the spinful SYK model shows the spontaneous breaking of a U(1) symmetry. However, rather than the breaking of an *axial* U(1) symmetry leading to a "traversable wormhole" phase [38–40], the *global* U(1) symmetry is instead broken, driving the system to a correlated spin-singlet superconducting phase. This superconductor shows an enhanced gap ratio compared to the BCS prediction, and might also exhibit connections to holography. It is separated by a first-order transition from a SYK non-Fermi liquid, in the vicinity of which a *gapless* superconducting phase, characterized by a finite magnetization, is stabilized upon applying a Zeeman field B (see a schematic low-temperature phase diagram in Fig. 1). Using a lattice construction with spinful SYK models at each site we compute the equilibrium transport properties of the two SC phases, finding sharp qualitative differences in their supercurrent-phase relations.

The model. We consider a variant of the SYK model that consists of a (0+1)-dimensional "quantum dot" with a large number N of degrees of freedom, each coming in two flavors $a = \uparrow, \downarrow$. We assume all-to-all random interactions between degrees of freedom of the same flavor, described by the complex SYK Hamiltonian,

$$H_a = \sum_{ijkl=1}^{N} J^a_{ij;kl} c^\dagger_{ia} c^\dagger_{ja} c_{ka} c_{la} - \mu_a \sum_j c^\dagger_{ja} c_{ja}, \tag{1}$$

where the coupling constants are drawn from a Gaussian distribution with zero mean and variance $\overline{|J^2_{ijkl}|} = \frac{J^2}{8N^3}$ and μ_a are chemical potentials that can be tuned independently for the two species. Fermionic commutation relations impose the constraints $J^a_{ij;kl} = -J^a_{ij;lk} = -J^a_{ji;kl} = (J^a_{kl;ij})^*$ on the coupling constants. In the following we also impose the stronger requirement that $J^a_{ij;kl}$ be fully antisymmetric [41]. We then require invariance under the antiunitary symmetry $\Theta = \tau^x \mathcal{K}$, where τ^x is a Pauli matrix acting on the flavor degree of freedom and $\mathcal{K}$ denotes complex conjugation. This enforces $J^\uparrow_{ij;kl} = (J^\downarrow_{ij;kl})^* = J^\downarrow_{kl;ij}$.

We now couple the cSYK models with two-body interactions that conserve charge for each flavor [with $U(1) \otimes U(1)$ symmetry] of the form $J^{ab}_{ijkl} c^\dagger_{ia} c^\dagger_{jb} c_{ka} c_{lb}$. Consistency with the antiunitary symmetry requires that $J^{ab}_{ijkl} = (J^{ba}_{ijkl})^*$. For concreteness we consider the coupling constants generated by

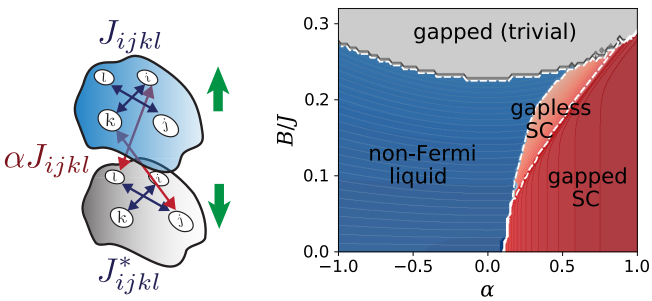

FIG. 1. (Left) Illustration of the coupling terms in the spinful SYK model, Eq. (2). (Right) Low-temperature ($\beta J = 100$) phase diagram as a function of Zeeman field B and interaction parameter α at charge neutrality $\mu = 0$. For $\alpha < 0$ the SYK non-Fermi liquid is stable, whereas for $\alpha > 0$ we find an instability to a gapped spin-singlet superconductor. Interestingly a region of gapless superconductivity with finite magnetization is stabilized at nonzero B. White dashed lines denote first-order phase transitions.

Coulomb interactions in a degenerate manifold that is constrained by Θ—see the Supplemental Material (SM) [42] for details and connections to a proposed physical platform based on a topological insulator flake. This enforces the constraints $J^{ab}_{il;kj} = \alpha J^{a}_{ij;kl} = \alpha J^{b}_{kl;ij}$ with α a dimensionless constant controlling the ratio of inter to intraflavor interactions. In the proposed physical platform $\alpha > 0$ ($\alpha < 0$) corresponds to repulsive (attractive) interflavor interactions. We thus consider

$$H = \sum_{ijkl} J_{ij;kl}[c^\dagger_{i\uparrow}c^\dagger_{j\uparrow}c_{k\uparrow}c_{l\uparrow} + c^\dagger_{k\downarrow}c^\dagger_{l\downarrow}c_{i\downarrow}c_{j\downarrow} + \alpha(c^\dagger_{i\uparrow}c^\dagger_{l\downarrow}c_{k\uparrow}c_{j\downarrow} + c^\dagger_{k\downarrow}c^\dagger_{j\uparrow}c_{i\downarrow}c_{l\uparrow})] - (\mu + B)\sum_j c^\dagger_{j\uparrow}c_{j\uparrow} - (\mu - B)\sum_j c^\dagger_{j\downarrow}c_{j\downarrow}, \quad (2)$$

where we expressed $\mu_{\uparrow,\downarrow} = \mu \pm B$ in terms of a (global) chemical potential μ and a Zeeman term B which breaks the antiunitary symmetry Θ. For $\mu = 0$ the Hamiltonian is invariant under the combination of flavor and particle-hole transformation $c^\dagger_{ia} \leftrightarrow c_{ib}$ with $a \neq b$.

Saddle-point equations. We first consider the charge neutrality point $\mu = 0$. The Euclidean-time path-integral formulation of the model at inverse temperature $\beta = 1/k_B T$ reads $\mathcal{Z} = \int[\mathcal{D}[c, c^\dagger]e^{-S}$ with the effective action $S = \int_0^\beta d\tau(\sum_{i,a} c^\dagger_{ia}(\tau)\partial_\tau c_{ia}(\tau) + H)$. Averaging over quenched disorder in the couplings J_{ijkl}, and considering only replica-diagonal solutions (assuming no spin-glass physics [43]), we obtain an effective action written in terms of the (standard and anomalous) averaged Green's functions $G_{\tau,\tau'} = \frac{1}{N}\sum_j\langle\mathcal{T}c_{j\uparrow}(\tau)c^\dagger_{j\uparrow}(\tau')\rangle$ and $F_{\tau,\tau'} = \frac{1}{N}\sum_j\langle\mathcal{T}c_{j\uparrow}(\tau)c_{j\downarrow}(\tau')\rangle$ and their respective self-energies Σ and Π (see the SM [42] for details). From this effective action the semiclassical ($N \to \infty$) saddle-point equations are obtained by taking functional derivatives with respect to the Green's functions and self-energies,

$$\Sigma_\tau = -J^2\left[\left(1 + \frac{\alpha^2}{2}\right)G^2_\tau G_{-\tau} - 2\alpha G_\tau F_\tau F_{-\tau} + \frac{\alpha^2}{2}F^2_\tau G_{-\tau}\right],$$
$$\Pi_\tau = -J^2\left[\left(1 + \frac{\alpha^2}{2}\right)F^2_\tau F_{-\tau} - 2\alpha F_\tau G_\tau G_{-\tau} + \frac{\alpha^2}{2}G^2_\tau F_{-\tau}\right],$$
$$G_n = -\frac{B + \Sigma_n + i\omega_n}{D_n}, \quad F_n = \frac{\Pi_n}{D_n}, \quad (3)$$

where $D_n = (B + \Sigma_n + i\omega_n)^2 - \Pi^2_n$. Here we used time translation invariance to express $G_{\tau,\tau'} \equiv G_{\tau-\tau'}$, whereas $G_n \equiv G(\omega_n)$ (and similarly) are Fourier-transformed expressions in terms of fermionic Matsubara frequencies $\omega_n = (2n + 1)\pi T$. This set of coupled equations can be solved self-consistently through an iterative method until convergence is attained. In practice, as coupled models of this type [36–40] often exhibit first-order phase transitions, we sweep the Zeeman field B back and forth and feed the converged solution for the next value of B considered. This gives rise to hysteresis curves from which one picks the solution with the lowest free-energy density $\mathcal{F} = -T\ \ln\ \mathcal{Z}/N$, given in the large-$N$ limit by substituting the saddle-point solutions in the action [44],

$$\frac{-\mathcal{F}}{T} = 2\ \ln\ 2 + \sum_{\omega_n}\left[\ln\left(\frac{D_n}{(i\omega_n)^2}\right) + \frac{3}{2}(\Sigma_n G_n + \Pi_n F_n)\right]. \quad (4)$$

Similarly, the entropy density $\mathcal{S} = (\mathcal{U} - \mathcal{F})/T$ is obtained, with the energy density

$$\mathcal{U} = T\sum_{\omega_n}[2BG_n + \Sigma_n G_n + \Pi_n F_n], \quad (5)$$

and the magnetization $M = \frac{1}{2N}\sum_j\langle c^\dagger_{j\uparrow}c_{j\uparrow} - c^\dagger_{j\downarrow}c_{j\downarrow}\rangle$ can be read off from $M = \frac{1}{2} - G_{\tau=0^+}$.

Phase diagram. We first explore the low-temperature physics of the model by self-consistently solving the saddle-point equations as described above. The resulting phase diagram is shown in Fig. 2. For attractive interactions between the two flavors ($\alpha < 0$) we find a SYK non-Fermi liquid with extensive residual entropy. In contrast, for repulsive interactions ($\alpha > 0$) there is an instability to a gapped superconducting phase generated by the spontaneous breaking of U(1) charge conservation. This should be compared to the results of Refs. [38,39], showing a spontaneous breaking of the *axial* U(1) symmetry with quantum number $Q_- = Q_\uparrow - Q_\downarrow$ whereby an "excitonic" order parameter $\frac{1}{N}\sum_j\langle c_{j\uparrow}c^\dagger_{j\downarrow}\rangle$ is generated for $\alpha < 0$. Indeed, the Hamiltonian studied in Refs. [38,39] is related to Eq. (2) by a particle-hole transformation for a single flavor $c^\dagger_{i\downarrow} \leftrightarrow c_{i\downarrow}$ combined with $\alpha \to -\alpha$, according to which we expect a spontaneous expectation value $\Delta \equiv F_{\tau=0} = \frac{1}{N}\sum_j\langle c_{j\uparrow}c_{j\downarrow}\rangle$ to develop for $\alpha > 0$. That is, in our case the *global* U(1) symmetry with $\mathcal{Q} = \mathcal{Q}_\uparrow + \mathcal{Q}_\downarrow$ is instead broken, leading to a spin-singlet SC state, and the instability now interestingly occurs for *repulsive* interflavor interactions.

In the presence of a weak Zeeman field B, the SC phase remains nonmagnetized ($M = 0$) as expected for a fully gapped spin-singlet superconductor. The breaking of time-reversal symmetry is however reflected in the different spectral gaps

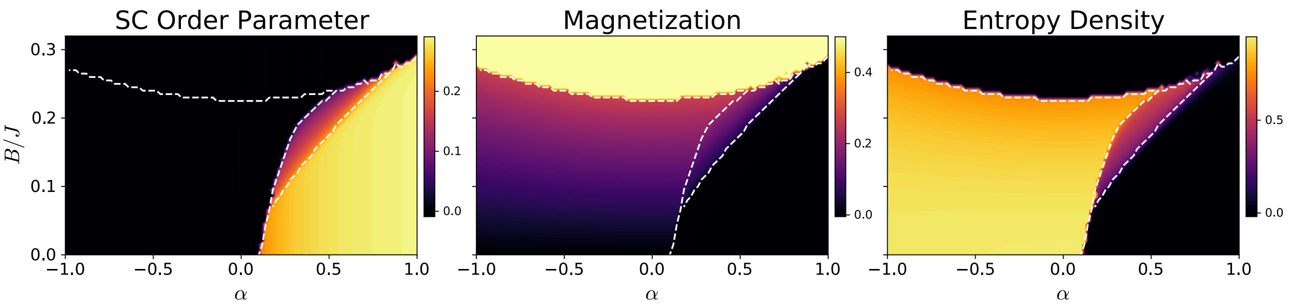

FIG. 2. Phase diagram of the model [Eq. (2)] at low-temperature $\beta J = 100$ and charge neutrality $\mu = 0$. The superconducting order parameter Δ (left panel), magnetization M (middle panel), and residual entropy density $\mathcal{S}_0$ (right panel) are obtained from the self-consistent solutions of Eqs. (3) as a function of α and B. Dashed white lines indicate first-order phase transitions.

for the hole and electron sides, as shown in Fig. 3. In contrast, the non-Fermi liquid phase can be continuously magnetized by tuning B, a reflection of the compressibility of the underlying cSYK models [12,35]. At sufficiently large B a first-order phase transition takes the system to a fully-polarized gapped state with $M = \frac{1}{2}$. The discontinuous jump in residual entropy between the non-Fermi liquid and gapped phases signals a first-order phase transition. The transition between the two gapped ordered phases (SC with $\Delta \neq 0$ and polarized phase with $M = \frac{1}{2}$) is also of first order as expected from standard Landau arguments.

A surprising result is the appearance of an intermediate phase which is gapless *and* superconducting, upon applying a Zeeman field B. This phase exhibits extensive residual entropy and magnetization associated with the SYK non-Fermi liquid as well as a nonzero SC order parameter Δ. The presence of a nonzero M and Δ seems contradictory but can occur, e.g., in a "phase coexistence" scenario where only part of the system spontaneously breaks the U(1) symmetry [38]. Here the Green's function G_τ exhibits power-law decay at long times, in contrast to the exponential decay observed in the gapped SC phase (see Fig. 3). When tuning the chemical potential away from charge neutrality ($\mu \neq 0$), we find that both the gapped and gapless SC phases are compressible as described the SM [42].

Gap ratio enhancement. We now increase temperature and consider the transition out of the gapped SC phase. In Fig. 4

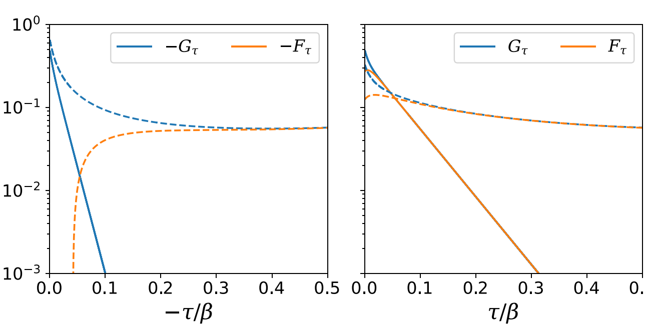

FIG. 3. Comparison of the regular and anomalous Green's functions G_τ and F_τ in the gapped (solid lines, $\alpha = 0.4$ and $B = 0.1J$) and gapless (dashed lines, $\alpha = 0.4$ and $B = 0.2J$) SC phases at low-temperature $\beta J = 200$. We show both negative (left) and positive (right) imaginary times τ.

we show the temperature dependence of Δ for $B = 0$. For large α we find that Δ smoothly goes to zero at T_c, indicative of a second-order transition, which is however not BCS-like as shown from comparing with the self-consistent solution of the BCS gap equations in the weak-coupling limit [1–3]. In particular, in BCS theory the following universal relations hold (with $k_B = 1$ and Δ_0 the SC order parameter at $T = 0$):

$$\Delta_0 = 1.76T_c, \quad \Delta(T \to T_c) = 3.06T_c\sqrt{1 - \frac{T}{T_c}}. \tag{6}$$

Here we find that neither relation is satisfied, highlighting the strongly correlated nature of superconductivity. Furthermore, the data collapse near T_c suggests that the SC transition becomes of first order when decreasing α. There is also a significant gap ratio enhancement [20] with Δ_0/T_c seemingly diverging for small α, which can be traced back to the empirical observation that $T_c \sim \alpha$ whereas Δ_0 depends only weakly on the interaction strength.

Equilibrium transport. We finally consider transport properties of the SC phases identified above. To do so we build a lattice model out of spinful SYK building blocks, connected by random hoppings similar to Ref. [18],

$$H = \sum_x H_x + \sum_{\langle x,x'\rangle} \sum_{ij\sigma} t_{ij\sigma}^{xx'} c_{i\sigma x}^\dagger c_{j\sigma x'}. \tag{7}$$

Here H_x describe spinful SYK models, Eq. (2), with an *independent* disorder realization on each site x. This ensures that the effective action only features local Green's functions and self-energies. The hopping terms connect nearest-neighbors $\langle x, x'\rangle$ and are drawn from a Gaussian distribution with zero mean and variance $\overline{|t_{ij\sigma}^{xx'}|^2} = \frac{t^2}{N}$.

To drive a supercurrent in the system we consider a ring geometry with L sites threaded by a magnetic flux Φ. This introduces Peierls phase factors in the hopping parameters through $t_{ij\sigma}^{xx'} e^{i\phi}$ with $\phi = \frac{e}{\hbar}\int \mathbf{A}\cdot d\mathbf{l} = \frac{2\pi}{L}\frac{\Phi}{\Phi_0}$ and the flux quantum $\Phi_0 = \frac{h}{e}$. If the hopping parameters are taken to be *uncorrelated* between the two spin components, the disorder average yields only the Green's function $G_{x,\tau}$ which is insensitive to the magnetic flux insertion. It is thus crucial to require invariance of the hopping terms under the antiunitary symmetry Θ—that is, $t_{ij\uparrow}^{xx'} = (t_{ij\downarrow}^{xx'})^*$. Combined with a translation-invariant ansatz whereby $G_{x,\tau} = G_\tau$ and $F_{x,\tau} = F_\tau$, we obtain saddle-point equations (see the SM [42]) that

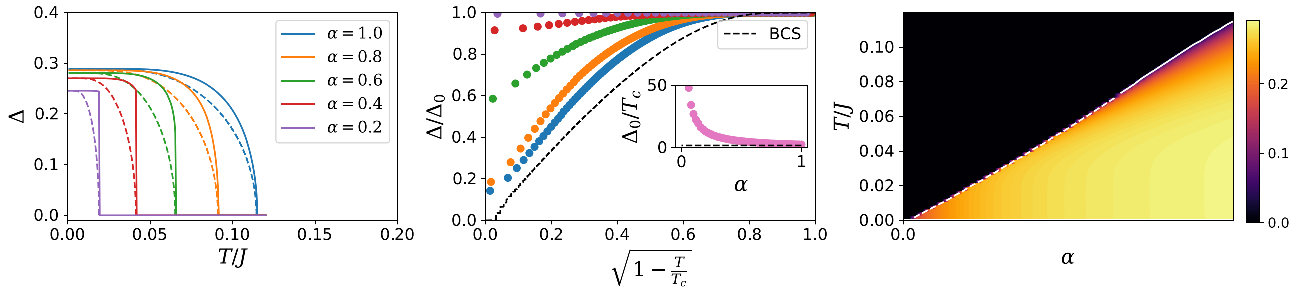

FIG. 4. (Left) Temperature dependence of the superconducting order parameter Δ for various values of α and $\mu = B = 0$. The weak-coupling BCS scaling is shown by dashed lines. (Middle) Data collapse of Δ/Δ_0 against $\sqrt{1 - T/T_c}$. There is a jump from a second- to a first-order phase transition when the interaction strength α decreases. (The inset) The ratio Δ_0/T_c increases as $\alpha \to 0$ and is greatly enhanced compared to the BCS result (dashed line). (Right) Phase diagram showing Δ in the T-α plane with second-order (solid line) and first-order (dashed line) phase transitions out of the gapped superconducting phase.

can be solved self-consistently. The free energy density $\mathcal{F}/L$ is computed using the appropriate generalization of Eq. (4), with the induced supercurrent

$$I = \frac{\partial \mathcal{F}}{\partial \Phi} = \frac{2e}{\hbar}\frac{\partial}{\partial \varphi}\left(\frac{\mathcal{F}}{L}\right), \tag{8}$$

where $\varphi = 2\phi$ is the phase carried by Cooper pairs when tunneling between SYK dots.

The limit of weak hopping t corresponds to Josephson tunneling between neighboring SC islands that are phase biased. Accordingly, we obtain sinusoidal supercurrent-phase relations $I(\varphi) = I_c \sin(\varphi + \delta)$ as shown in Fig. 5 for $\alpha = 0.5$ and various values of B. In the gapped phase we find $\delta = 0$ and the maximal supercurrent $I_c \sim t^2/J$, as expected in perturbation theory from the tunneling of Cooper pairs between neighboring sites. For sufficiently large B the gapless SC phase is stabilized (see also Fig. 2), which in transport is manifest as a phase-shifted supercurrent relation with $\delta = \pi$. In other words, the system's free energy is minimized for a staggered order parameter Δ_x with a π-phase difference

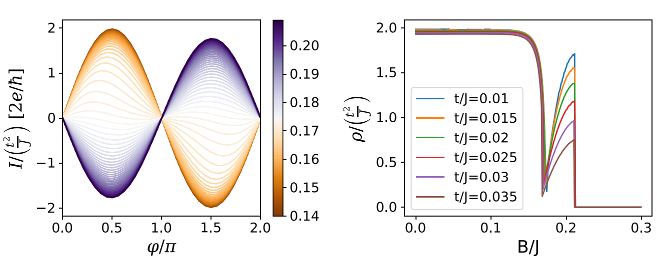

FIG. 5. Equilibrium transport properties of the two superconducting phases, here for $\alpha = 0.5$. (Left) Supercurrent-phase relation $I(\varphi)$ [computed through Eq. (8)] in the lattice model for various values of the Zeeman field B/J (color scale) and $t/J = 0.01$. The jump to a π-shifted sinusoidal profile coincides with the first-order transition between the gapped and gapless SC phases at the critical Zeeman field B_c. (Right) The superfluid density ρ (in arbitrary units) is independent of B in the gapped phase and shows a recovery after a sudden drop at B_c.

between neighboring sites. The superfluid density $\rho \sim \frac{\partial I}{\partial \varphi}|_{\varphi\to\delta}$ is independent of B in the gapped phase but interestingly shows a recovery with B in the gapless phase, following a sudden drop at the phase transition at B_c. The gapless SC phase is also more fragile to competing energy scales as seen from the rapid decrease in ρ/t^2 as a function of t.

Discussion. In this Letter we introduced a simple "spinful SYK" model for strongly correlated superconductivity. Its exact solvability in the large-N limit allowed us to map the model's phase diagram which exhibits *two* different (gapped and gapless) superconducting phases and show how their behavior strongly deviates from BCS theory. The transport properties of such phases, going beyond the equilibrium picture presented here, could be explored in future work. Indeed, the lattice model in Eq. (7) hosts not only correlated SC phases, but also a strange metal and a heavy Fermi liquid (depending on the ratio t/J) in the limit $\alpha = 0$ where it reduces to two decoupled (spinless) SYK chains [18]. It would be interesting to study the thermal and electrical conductivity across this rich phase diagram, which bears some resemblance to the phenomenology of cuprates.

To summarize, this Letter adds to the growing body of literature on SYK superconductivity [25–34] by highlighting the role of antiunitary symmetries in promoting SC instabilities. Furthermore, the model's simple structure and connections to physical platforms where superconducting instabilities are expected for *repulsive electronic interactions* raise the hope of stimulating new experimental developments. An interesting open question concerns the effect of (finite-N) fluctuations away from the saddle point, which should restore the broken U(1) symmetry at low energy in accordance with the Mermin-Wagner theorem [14,45].

Acknowledgments. We are grateful to S. Plugge for discussions and collaborations on related projects and to N. Gnezdilov and Y. Wang for insightful comments on the first version of this Letter. This research was supported, in part, by the National Sciences and Engineering Research Council of Canada (NSERC) and the Canada First Research Excellence Fund (CFREF).

[1] J. Bardeen, L. N. Cooper, and J. R. Schrieffer, Microscopic theory of superconductivity, Phys. Rev. **106**, 162 (1957).
[2] J. Bardeen, L. N. Cooper, and J. R. Schrieffer, Theory of superconductivity, Phys. Rev. **108**, 1175 (1957).
[3] L. P. Gor'Kov, On the energy spectrum of superconductors, Sov. Phys. JETP **7**, 158 (1958).
[4] A. B. Migdal, Interaction between electrons and lattice vibrations in a normal metal, Sov. Phys. JETP **7**, 996 (1958).
[5] G. M. Eliashberg, Interactions between electrons and lattice vibrations in a superconductor, Sov. Phys. JETP **11**, 696 (1960).
[6] Y. Nambu, Quasi-particles and gauge invariance in the theory of superconductivity, Phys. Rev. **117**, 648 (1960).
[7] F. Marsiglio, Eliashberg theory: A short review, Ann. Phys. **417**, 168102 (2020).
[8] P. W. Phillips, L. Yeo, and E. W. Huang, Exact theory for superconductivity in a doped mott insulator, Nat. Phys. **16**, 1175 (2020).
[9] G.-Z. Liu, Z.-K. Yang, X.-Y. Pan, and J.-R. Wang, Towards exact solutions for the superconducting T_c induced by electron-phonon interaction, Phys. Rev. B **103**, 094501 (2021).
[10] V. Crépel and L. Fu, New mechanism and exact theory of superconductivity from strong repulsive interaction, arXiv:2012.08528.
[11] S. Sachdev and J. Ye, Gapless Spin-Fluid Ground State in a Random Quantum Heisenberg Magnet, Phys. Rev. Lett. **70**, 3339 (1993).
[12] S. Sachdev, Bekenstein-Hawking Entropy and Strange Metals, Phys. Rev. X **5**, 041025 (2015).
[13] A. Kitaev, A simple model of quantum holography, in KITP Strings Seminar and Entanglement 2015 Program, Kavli Institute for Theoretical Physics, 2015, https://online.kitp.ucsb.edu/online/entangled15/kitaev/ and https://online.kitp.ucsb.edu/online/entangled15/kitaev2/.
[14] J. Maldacena and D. Stanford, Remarks on the Sachdev-Ye-Kitaev model, Phys. Rev. D **94**, 106002 (2016).
[15] S. Banerjee and E. Altman, Solvable model for a dynamical quantum phase transition from fast to slow scrambling, Phys. Rev. B **95**, 134302 (2017).
[16] S.-K. Jian and H. Yao, Solvable Sachdev-Ye-Kitaev Models in Higher Dimensions: From Diffusion to Many-Body Localization, Phys. Rev. Lett. **119**, 206602 (2017).
[17] Y. Gu, X.-L. Qi, and D. Stanford, Local criticality, diffusion and chaos in generalized Sachdev-Ye-Kitaev models, J. High Energy Phys. 05 (2017) 125.
[18] X.-Y. Song, C.-M. Jian, and L. Balents, Strongly Correlated Metal Built from Sachdev-Ye-Kitaev Models, Phys. Rev. Lett. **119**, 216601 (2017).
[19] Z. Bi, C.-M. Jian, Y.-Z. You, K. A. Pawlak, and C. Xu, Instability of the non-fermi-liquid state of the Sachdev-Ye-Kitaev model, Phys. Rev. B **95**, 205105 (2017).
[20] A. A. Patel, J. McGreevy, D. P. Arovas, and S. Sachdev, Magnetotransport in a Model of a Disordered Strange Metal, Phys. Rev. X **8**, 021049 (2018).
[21] D. Chowdhury, Y. Werman, E. Berg, and T. Senthil, Translationally Invariant Non-Fermi-Liquid Metals with Critical Fermi Surfaces: Solvable Models, Phys. Rev. X **8**, 031024 (2018).
[22] X. Wu, X. Chen, C.-M. Jian, Y.-Z. You, and C. Xu, Candidate theory for the strange metal phase at a finite-energy window, Phys. Rev. B **98**, 165117 (2018).
[23] P. Cha, N. Wentzell, O. Parcollet, A. Georges, and E.-A. Kim, Linear resistivity and Sachdev-Ye-Kitaev (SYK) spin liquid behavior in a quantum critical metal with spin-1/2 fermions, Proc. Natl. Acad. Sci. USA **117**, 18341 (2020).
[24] J. Kim, X. Cao, and E. Altman, Low-rank Sachdev-Ye-Kitaev models, Phys. Rev. B **101**, 125112 (2020).
[25] A. A. Patel, M. J. Lawler, and E.-A. Kim, Coherent Superconductivity with a Large Gap Ratio From Incoherent Metals, Phys. Rev. Lett. **121**, 187001 (2018).
[26] Y. Cheipesh, A. I. Pavlov, V. Scopelliti, J. Tworzydło, and N. V. Gnezdilov, Reentrant superconductivity in a quantum dot coupled to a Sachdev-Ye-Kitaev metal, Phys. Rev. B **100**, 220506(R) (2019).
[27] H. Wang, A. L. Chudnovskiy, A. Gorsky, and A. Kamenev, Sachdev-Ye-Kitaev superconductivity: Quantum Kuramoto and generalized Richardson models, Phys. Rev. Research **2**, 033025 (2020).
[28] I. Esterlis and J. Schmalian, Cooper pairing of incoherent electrons: An electron-phonon version of the Sachdev-Ye-Kitaev model, Phys. Rev. B **100**, 115132 (2019).
[29] Y. Wang, Solvable Strong-Coupling Quantum-Dot Model with a Non-Fermi-Liquid Pairing Transition, Phys. Rev. Lett. **124**, 017002 (2020).
[30] Y. Wang and A. V. Chubukov, Quantum phase transition in the Yukawa-Syk model, Phys. Rev. Research **2**, 033084 (2020).
[31] D. Hauck, M. J. Klug, I. Esterlis, and J. Schmalian, Eliashberg equations for an electron–phonon version of the Sachdev–Ye–Kitaev model: Pair breaking in non-fermi liquid superconductors, Ann. Phys. **417**, 168120 (2020).
[32] G. Pan, W. Wang, A. Davis, Y. Wang, and Z. Y. Meng, Yukawa-syk model and self-tuned quantum criticality, Phys. Rev. Research **3**, 013250 (2021).
[33] D. Chowdhury and E. Berg, Intrinsic superconducting instabilities of a solvable model for an incoherent metal, Phys. Rev. Research **2**, 013301 (2020).
[34] D. Chowdhury and E. Berg, The unreasonable effectiveness of eliashberg theory for pairing of non-fermi liquids, Ann. Phys. **417**, 168125 (2020).
[35] Y. Gu, A. Kitaev, S. Sachdev, and G. Tarnopolsky, Notes on the complex Sachdev-Ye-Kitaev model, J. High Energy Phys. 02 (2020) 157.
[36] J. Maldacena and X.-L. Qi, Eternal traversable wormhole, arXiv:1804.00491.
[37] J. Kim, I. R. Klebanov, G. Tarnopolsky, and W. Zhao, Symmetry Breaking in Coupled SYK or Tensor Models, Phys. Rev. X **9**, 021043 (2019).
[38] S. Sahoo, É. Lantagne-Hurtubise, S. Plugge, and M. Franz, Traversable wormhole and Hawking-Page transition in coupled complex SYK models, Phys. Rev. Research **2**, 043049 (2020).
[39] I. R. Klebanov, A. Milekhin, G. Tarnopolsky, and W. Zhao, Spontaneous breaking of U(1) symmetry in coupled complex SYK models, J. High Energy Phys. 11 (2020) 162.
[40] A. M. García-García, J. P. Zheng, and V. Ziogas, Phase diagram of a two-site coupled complex SYK model, Phys. Rev. D **103**, 106023 (2021).
[41] In the large-N limit such fully antisymmetric terms are expected to dominate, as their number scales as $\sim N^4$, rather than N^3 or N^2 for interaction terms with one or two repeated indices. In mesoscopic systems, these omitted terms could however play an important role.

[42] See Supplemental Material at http://link.aps.org/supplemental/10.1103/PhysRevB.104.L020509 which presents connections to proposed physical platforms, details of effective action calculations, and additional numerical results. It also includes Refs. [46–51].

[43] In the context of SYK physics, replica off-diagonal solutions are believed to be subleading in the large-N limit [52–55]. An extension of this analysis to the spinful SYK model is beyond the scope of the present paper.

[44] Here we regularized the free energy (divided by T) using its value for $2N$ noninteracting complex fermions, $2\sum_n \ln(i\omega_n) = 2\ln 2$, to regularize divergences at large frequencies in the numerical evaluation of D_n.

[45] D. Bagrets, A. Altland, and A. Kamenev, Sachdev–Ye–Kitaev model as Liouville quantum mechanics, Nucl. Phys. B **911**, 191 (2016).

[46] A. Chen, R. Ilan, F. de Juan, D. I. Pikulin, and M. Franz, Quantum Holography in a Graphene Flake with an Irregular Boundary, Phys. Rev. Lett. **121**, 036403 (2018).

[47] I. Danshita, M. Hanada, and M. Tezuka, Creating and probing the Sachdev-Ye-Kitaev model with ultracold gases: Towards experimental studies of quantum gravity, Prog. Theor. Exp. Phys. **2017**, 083I01 (2017).

[48] C. Wei and T. A. Sedrakyan, Optical lattice platform for the Sachdev-Ye-Kitaev model, Phys. Rev. A **103**, 013323 (2021).

[49] P. Cheng, C. Song, T. Zhang, Y. Zhang, Y. Wang, J.-F. Jia, J. Wang, Y. Wang, B.-F. Zhu, X. Chen, X. Ma, K. He, L. Wang, X. Dai, Z. Fang, X. Xie, X.-L. Qi, C.-X. Liu, S.-C. Zhang, and Q.-K. Xue, Landau Quantization of Topological Surface States in Bi_2Se_3, Phys. Rev. Lett. **105**, 076801 (2010).

[50] R. Yoshimi, A. Tsukazaki, Y. Kozuka, J. Falson, K. S. Takahashi, J. G. Checkelsky, N. Nagaosa, M. Kawasaki, and Y. Tokura, Quantum Hall effect on top and bottom surface states of topological insulator $(Bi_{1-x}Sb_x)_2Te_3$ films, Nat. Commun. **6**, 6627 (2015).

[51] T.-G. Zhou, L. Pan, Y. Chen, P. Zhang, and H. Zhai, Disconnecting a traversable wormhole: Universal quench dynamics in random spin models, Phys. Rev. Research **3**, L022024 (2021).

[52] A. Kitaev and S. Josephine Suh, The soft mode in the Sachdev-Ye-Kitaev model and its gravity dual, J. High Energy Phys. 05 (2018) 183.

[53] H. Wang, D. Bagrets, A. L. Chudnovskiy, and A. Kamenev, On the replica structure of Sachdev-Ye-Kitaev model, J. High Energy Phys. 09 (2019) 057.

[54] I. Aref'eva, M. Khramtsov, M. Tikhanovskaya, and I. Volovich, Replica-nondiagonal solutions in the SYK model, J. High Energy Phys. 07 (2019) 113.

[55] C. L. Baldwin and B. Swingle, Quenched vs Annealed: Glassiness from SK to SYK, Phys. Rev. X **10**, 031026 (2020).